



Available online at [www.academicpaper.org](http://www.academicpaper.org)

**Academic @ Paper**

ISSN 2146-9067

International Journal of Automotive  
Engineering and Technologies

Vol. 5, Issue 2, pp. 53 – 60, 2016

**International Journal of Automotive  
Engineering and Technologies**

<http://www.academicpaper.org/index.php/IJAET>

**Original Research Article**

## **The Determination of Aerodynamic Drag Coefficient of Truck and Trailer Model by Wind Tunnel Tests**

Cihan Bayındırlı<sup>1</sup>, Y. Erkan Akansu<sup>2</sup> M. Sahir Salman<sup>3</sup>

<sup>1</sup>Nigde Vocational School of Technical Sciences, Niğde University, 51000, Niğde, Turkey

<sup>2</sup>Niğde University, Faculty of Engineering, Mechanical Engineering Department, 51000 Niğde, Turkey

<sup>3</sup>Gazi University, Faculty of Technology, Automotive Engineering Department, 06500, Ankara, Turkey

Received 28 March 2016 Accepted 20 June 2016

### **Abstract**

In this study, surface pressure and drag measurements were conducted for a heavy vehicle model consisted of 1/32 scaled truck and trailer which was placed in a wind tunnel. The wind tunnel tests of truck trailer combination were carried out in the range of 117 000 - 844 000 Reynolds numbers. The pressure coefficient ( $C_p$ ) distribution and aerodynamic drag coefficient ( $C_D$ ) on truck and trailer were experimentally determined. The regions forming aerodynamic drag on the truck trailer was determined at the result of the flow visualization. The average drag coefficient ( $C_D$ ) was determined as 0.608 for truck. The drag coefficients was obtained as 0.704 for truck trailer combination. The drag coefficient ( $C_D$ ) increased 15.8%, when the trailer was attached to the truck.

**Keywords:** The aerodynamic drag coefficient, wind tunnel, aerodynamic, drag force, pressure coefficient, and drag force

Doi: 10.18245/ijaet.11754

\*Corresponding Author:

E-mail: [cbayindirli@nigde.edu.tr](mailto:cbayindirli@nigde.edu.tr)

## 1. Introduction

One of the forces acting on the vehicle is aerodynamic drag force. Aerodynamic drag force becomes important at higher speeds and vehicle performance and fuel consumption are significantly influenced. Because the aerodynamic drag force increases proportional to the square of the speed. The heavy vehicles perform cruising at high speed in intercity and take way too much over the years. The vehicle manufacturers invest aerodynamic studies in order to increase vehicle performance. It is seen on the shape in Fig. 1 shape that forming aerodynamic drag regions on heavy vehicles. A large amount of drag based on pressure drag is consisted on the front surface, the wheels, the gap between the truck and trailer and the rear of the trailer [20].

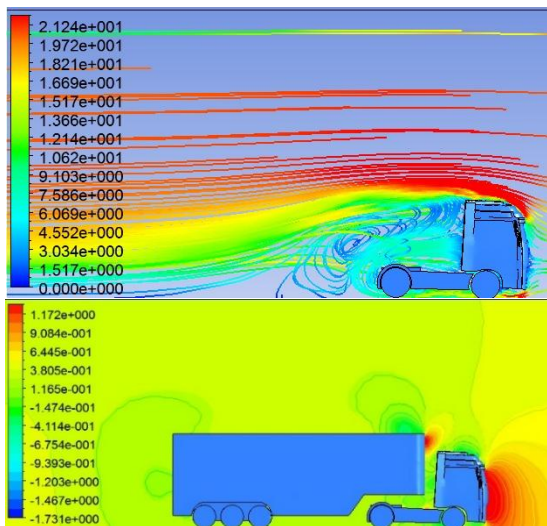


Fig. 1 The high pressure drag regions on heavy vehicles [20]

The aerodynamics is called as a science branches that investigates external flow the interaction of moving of solid structures or bodies with the air. The aerodynamic drag coefficient significantly affect the vehicle's performance, fuel consumption, acceleration properties, handling characteristics, environmental pollution, noise and comfort [1, 2, 3, 4, and 5]. Moreover, the cooling system of engine and the heating interior ventilation system have a direct relationship with the aerodynamics. The drag force is increased proportionally with the square of the speed. [6, 7, 8]. This status makes the

improving aerodynamics drag more important issue for heavy vehicles which perform a large part of the transportation out of the city and a lot of miles at high speeds for a year. A passenger car with 100 km speed an hour spends 60% of its power to afford the forces of drag [2]. Considerable savings is achieved from the fuel consumption with the improvement of the aerodynamic properties of the vehicle [10, 11, 12 and 14]. The passive and active flow control methods are used to improve the aerodynamics of the car. Perzon, and Davidson provided the aerodynamic improvements with three different models that they made. By rounding the back of the trailer he achieved 4 % improvement. He stated that he made 3% improvements with nose cone and 7% improvements with chassis skirt [13]. The aerodynamic drag coefficients of 1/24 scale BMW X5 E53, Alfa Romeo 156 ve Wolkswagen New Beetle model cars were found with 14%, 12.5%, 7.8% difference rate at 28 m/s wind tunnel speed [15]. With increasing windshield attack angle drag coefficient decreases on a commercial vehicles [16]. Modi and others aerodynamic improvement is obtained on 1/6 scale a truck and trailer model. The vertical and horizontal spoiler put at the front of the trailer have achieved to improve by 12.5% and 28% respectively [17]. A large part of the aerodynamic drag is formed on the front surface area of truck. The drag coefficient is approximately 0.6 of truck and trailer [18]. According to Ogburn and Ramroth a decrease of 20 % in drag force is obtainable by adding some aerodynamic part on truck and trailer. The improvement in that ratio decrease fuel consumption about 10 % at or over 105 km / h speed [19]. Ozel and others (2011) obtained 23.15 % aerodynamic improvement by passive flow control methods [20]. Akansu and others obtained % 25.58 aerodynamic improvement using passive flow control parts on truck trailer model. They used better designed spoiler, passive air channel and two different model air redirector [21].

The aim of this study is to examine the aerodynamics structures of truck and trailer

combinations and determine of zones which forms aerodynamic drag as experimentally. To view and investigate the flow around the truck and trailer by flow visualization methods.

## 2. Material Methods

The size of suction type wind tunnel test region is 400mm x 400mm x 1000mm. The rpm of the fan motor was been controlled to achieve the desired free stream in the test region by using frequency inverter. The frequency inverter operates in the range of 0-50 Hz and has 0.1 Hz step, to control 4 kW powered axial fan of 700 mm diameter. A six-component load cell has been used to measure  $F_x$  and  $F_y$  forces up to  $\pm 32N$  and  $F_z$  force up to  $\pm 100N$ . It can measure  $M_x$ ,  $M_y$ ,  $M_z$  moments in the range of  $\pm 2.5Nm$ . Turbulence intensity is below 1% in the wind tunnel.

The wind tunnel tests were carried out in the range of 117 000 - 844 000 Reynolds numbers. The minimum and maximum free velocity in the range of 0-28 m/s. The blocking rate is 8.31 %. The view of the test devices and wind tunnel is given in Fig. 2.



Fig. 2. General view of the test devices and wind tunnel



Fig. 3. 1/32 Scaled model vehicle

### 2.1. Description of Model

Table 1. The Features of Model Vehicle

Body and Chassis: Diecast metal,
Bumper, Mirrors, Trailer and Glass: Plastic
Appearance: Metallic Blue, Grey Painted, Smooth
Sizes of Truck-Trailer Height: 16.17 cm Width: 9.2 cm, Length (L): 48.878 cm
Characteristics Area of Truck-Trailer (A) : 0,0132 m <sup>2</sup>
Characteristics Area of Truck (A) : 0,0108 m <sup>2</sup>

### 2.2. The Tests of Pressure Measurement

A total of 32 taps were located symmetry axis of the vehicle, 13 taps of which on the truck and 19 taps of which on the trailers, have been used. The pressure measurements of truck were conducted in the range of 117 000 - 317 000 Reynolds number and tests of truck trailer combination were carried out in the range of 312 000 - 844 000 Reynolds number.

Dynamic pressure which was used obtained from the pressure taps on the inlet and outlet of the wind tunnel contraction cone. Two differential type pressure converter is used in the pressure measurements. It is Omega PX163-2.5BD5V model, the output voltage of 0-5 volts detection time is 1 milisecond. Before the pressure measurements, the calibration of pressure transducers is made. The determining of surface pressure, 800 data is received in a second, this value is below of the detection time capacity of the pressure transducer (1000 Hz). Total of 16 384 data has been taken and each measurement taken is 20.48 seconds.

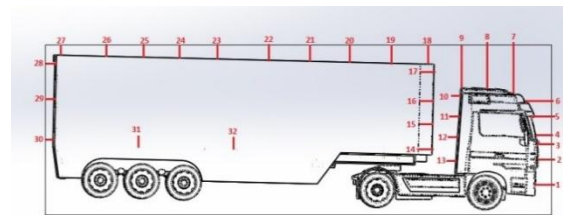


Fig. 4. The location of the pressure probe on model car

The difference between total pressure and static pressure gives the dynamic pressure.

$$P_{dyn} = P_{total} - P_{st} \quad (1)$$

$$P_{dyn} = \frac{1}{2} \rho V^2 \quad (2)$$

$$C_P = \frac{\Delta P}{\frac{1}{2}\rho V^2 A} \quad (3)$$

In the experimental studies, atmospheric pressure, dynamic pressure, free stream velocity and ambient temperature were measured with a Mano air 500 model digital micro manometer.

### 2.3. The Force Measurement Tests

Aerodynamic drag coefficient is expressed with the parameters of drag force  $F_D$ , the density of air  $\rho$ , the free stream velocity  $V$  and as the front projection area of vehicle  $A$ .

$$C_D = \frac{F_D}{\frac{1}{2}\rho V^2 A} \quad (4)$$

The measurement of drag forces was carried out a six-axis load cell which is ATI brand Gamma model. Load cell can measure  $F_x$  and  $F_y$  forces up to  $\pm 32N$  and  $F_z$  force up to  $\pm 100N$ . It can measure  $M_x$ ,  $M_y$ ,  $M_z$  moments in the range of  $\pm 2.5Nm$ . The force measurements were made 6 different speeds (5 m/s, 10 m/s, 15 m/s, 20 m/s, 25 m/s, 27 m/s). During the one minute two results have been taken per second. The drag coefficient has been calculated based on a total of 120 results.

### 2.4. Establishing of Similarities Rules for Study

The experimental studies related to vehicle aerodynamics on real prototypes are quite expensive and difficult. So, scaled model vehicles can be used in the wind tunnel experiments. Three different similarities are required between prototypes.

#### 2.4.1. Geometric Similarity

To ensure geometric similarity, the sizes of model should be proportional to that of the prototype. In the wind tunnel tests 1/32 scaled model vehicle is used. It is a licensed model and the error has been neglected depends on the surface roughness.

#### 2.4.2. Kinematic Similarity

The ratios of the velocity vector on prototypes and models should be same to provide kinematic similarity [8]. Providing kinematic similarity also depends on blocking effect in the wind tunnel

experiments. Blockage ratio is defined as projection area of the front surface of the model, proportional to area of the front surface of wind tunnel test section. In the literature, blockage ratio is recommended to be below the 10 % limit for the blocking effect to be neglected in wind tunnel tests [2]. In this study, blocking ratio is 8.31%. As this value is in accordance with the criteria given in the literature, the effects of blockade have been neglected.

#### 2.4.3. Dynamic Similarity

Reynolds number is defined as the ratio of inertial forces to viscous forces.

$$Re = U_\infty L/\nu \quad (5)$$

Reynolds number must be the same for model and prototype in the studies where inertia and viscous forces are effective force to ensure full dynamic similarity.

However, unless models and prototypes aren't in the same size, it is very difficult to achieve equality in the numbers of Reynolds. Dimensionless coefficients above a certain speed value may not be affected by the Reynolds number.

Due to the Reynolds number independence the dynamic similarity can be assumed as provided for the flow over bluff bodies like trucks and buildings. The drag coefficient may not change after a threshold value of Reynolds number. In the case of the boundary layer and the wake are fully turbulent [7]. In Fig. 5, Reynolds number independence was obtained in wind tunnel tests.

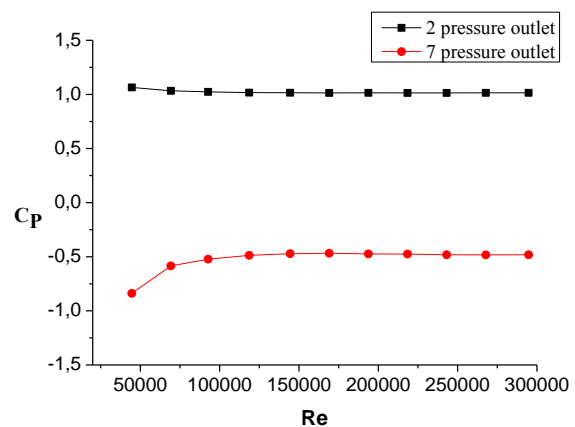


Fig.5. Reynolds independent in tests

## 2.5. Uncertainty Analysis

In this study the results of the uncertainty analysis of the calculated parameters are given below.

### 2.5.1. Calculation of the uncertainty value of the Reynolds number

Uncertainty value for the Re number were obtained as 1.3%.by writing  $\rho$ ,  $U_{Pitot}$ ,  $H$  and  $\mu$  argument of uncertainty values instead of equation 6.

$$u_{Re} = \frac{w_{Re}}{Re} = \left[ (u_{\rho})^2 + (u_{Pitot})^2 + (u_H)^2 + (u_{\mu})^2 \right]^{1/2} \quad (6)$$

### 2.5.2. Calculation of the uncertainty value of the drag force

The uncertainty values that is acting coefficient of drag forces was obtained as 4.5%. It was calculated for  $U = 10 \text{ m/s}$  and  $Re = 312\,000$  value.

$$\frac{w_{FD}}{F_D} = \left[ \left( \frac{w_{X_1}}{X_1} \right)^2 + \left( \frac{w_{X_2}}{X_2} \right)^2 + \left( \frac{w_{X_3}}{X_3} \right)^2 + \left( \frac{w_{X_4}}{X_4} \right) \left( \frac{w_{X_4}}{X_4} \right) + \left( \frac{w_{X_5}}{X_5} \right)^2 \right]^{1/2} \quad (7)$$

### 2.5.3. Calculation of the uncertainty value of the aerodynamic drag coefficient

The uncertainty value for the aerodynamic force coefficient were obtained as 4.7%.by writing  $F$ ,  $\rho$ ,  $A$ , argument of uncertainty values instead of equation 8.

$$u_{CD} = \frac{w_{CD}}{C_D} = \left[ (u_{FD})^2 + (u_{\rho})^2 + 4(u_{pitot})^2 + (u_{A_{\delta n}})^2 \right]^{1/2} \quad (8)$$

### 2.5.4. Calculation of the uncertainty value of the pressure coefficient ( $C_P$ )

The Uncertainty value for the pressure coefficient ( $C_P$ ) were obtained as 2.11 %.by writing  $\Delta P$ ,  $\rho$  and  $U$  argument of uncertainty values instead of equation 9.

$$u_{C_P} = \frac{w_{C_P}}{C_P} = \left[ (u_{\Delta P})^2 + (u_{\rho})^2 + 4(u_{pitot})^2 \right]^{1/2} \quad (9)$$

## 3. Result and Discussion

### 3.1. Pressure Coefficient ( $C_P$ ) Distribution on Truck

According to results of pressure measurements, the highest pressure value was obtained on the pressure tap 2 and 3. It was established that stagnation pressure has occurred between these two taps. The distribution of  $C_P$  on the truck is given in Fig.6.

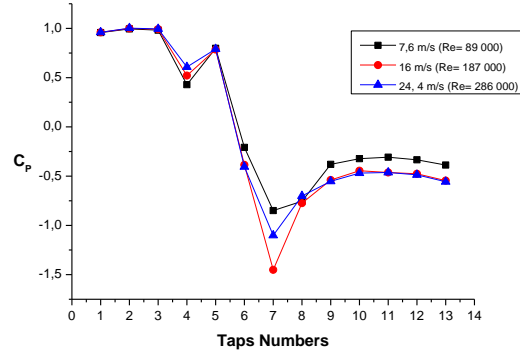


Fig. 6. The pressure coefficient ( $C_P$ ) distribution on the truck

### 3.2. Pressure Coefficient ( $C_P$ ) Distribution on Truck and Trailer

Especially, the pressure coefficient values have been found as high on the 17,18 and 19 taps due to the fact that trailer is higher than the truck. The pressure coefficient ( $C_P$ ) was found to be 0.96 on the probe18. It has been seen in Fig. 7, the pressure coefficient on the tap 18 has a value of 0.96 which is close to stagnation pressures. The separated flow over spoiler has reattached on the trailer where higher region than truck.

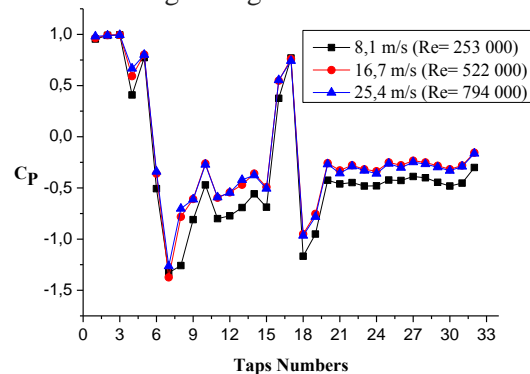


Fig. 7. The pressure coefficient ( $C_P$ ) distribution on the truck trailer combination

### 3.3. The drag force measurements of truck

As a result of the experiments is given Table 3.1. The average drag coefficient ( $C_D$ ) of truck was determined as 0.608. When analyzing the distribution of pressure coefficient, it is seen that the drag coefficient

can be decreased and especially with improvements of bumper, spoiler design and inclination windshield angle.

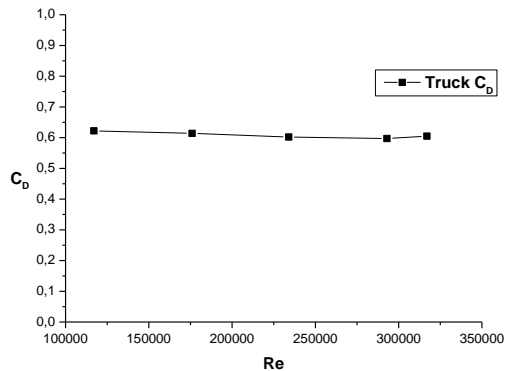


Fig. 8. The drag coefficient graphic of truck

Table 3.1. The measured force and  $C_D$  values of truck

Reynolds Number	Force (N)	$C_D$
117 000	0,337	0,622
176 000	0,749	0,614
234 000	1,305	0,602
293 000	2,022	0,597
317 000	2,389	0,605

It is observed in Fig. 8, because of negative pressure area is large rear of truck, it causes an increase of drag coefficient.



Fig.9. Flow visualization of truck

### 3.4. The drag force measurements of truck and trailer

As seen Table 3.2, the average aerodynamic drag coefficient of truck and trailer was measured as 0.704.

Table 3.2. The measured force and  $C_D$  values of truck and trailer

Reynolds Number	Force (N)	$C_D$
312 000	0,467	0,707
469 000	1,036	0,697
625 000	1,889	0,714
781 000	2,917	0,706
844 000	3,359	0,697

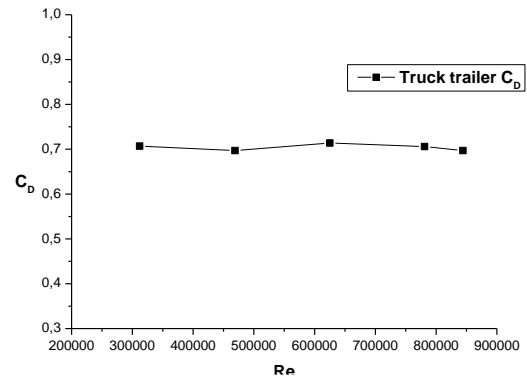


Fig. 9. The drag coefficient graphic of truck trailer

The drag coefficient ( $C_D$ ) increased 15.8%, when the trailer was attached to the truck. When analyzing the graph of pressure distribution, it is seen that pressure coefficient is high and the spoiler and the aerodynamic improvements can be made in the front upper part of the trailer where probe 17 and 18 are. Also, aerodynamic structure is negatively affected due to negative pressure region between truck and trailer. It has been determined the aerodynamic structure can be improved by reducing the incoming air entering to the negative pressure region.



Fig.10. Flow visualization of truck and trailer

### 4. Conclusion and Recommendations

In this study the flow structure on the truck trailer model, the forces acting on the vehicle values were determined experimentally in a wind tunnel. The experimental studies are made at Reynolds numbers in the range of 117 000-844 000. The effect of added the trailer to aerodynamic drag coefficient was determined. It was observed flow in visualization and distribution of pressure coefficient that the pressure coefficients is very high on the front bumper and windshield. Front shape of the truck should

be designed more curved and narrow windshield inclination in order to reduce aerodynamic drag. The attached trailer to truck has increased the drag coefficient ( $C_D$ ) as 15.80%. The trailers must be selected according to the geometric shape and size of the truck.

## 5. References

1. Wood, R.M. and Bauer, S.X.S. (2003). Simple and low cost aerodynamic drag reduction devices for tractor-trailer Trucks. SAE Technical Paper, 01-3377, 1-18.
2. Çakmak, M.A., "Investigation of vehicles as aerodynamically", *Mühendis Makina*, 41, 489, 2000.
3. Wahba, C. E.M., Al-Marzooqi, H., Shaath, M., Shahin, M., and El-Dhmarshawy. T. (2012). Aerodynamic Drag Reduction for Ground Vehicles using Lateral Guide Vanes. *CFD Letters* Vol. 4(2), 68-78.
4. Gilhaus, A, "The influence of cab shape on air drag of trucks", *Journal of Wind Engineering and Industrial Aerodynamics*, 9, 77-87, 1981.
5. Chowdhury, H, Moria H, Ali A, Khan I, Alam, F, Watkins, S, "A study on aerodynamic drag of a semi-trailer truck" 5th BSME International Conference on Thermal Engineering Volume 56, Pages 201-205, 2013.
6. Miralbes, R, "Analysis of Some Aerodynamic Improvements for Semi-Trailer Tankers" Proceedings of the World Congress on Engineering Vol 3 WCE, 4-6 July, London U.K, 2012.
7. Çengel, A, Y, Cimbala J, M, "Fluid Mechanics Fundamentals and Applications", (Translator. Tahsin Engin, H. Rıdvan Öz, Hasan Küçük, Şevki Çeşmeci), Güven Bilimsel, İzmir, 2008.
8. Sahin C, "Prediction of Aerodynamic Drag Coefficient for Heavy Vehicles with Computational Fluid Dynamics Method" İstanbul Technical University, Institute of Science and Technology, Master Thesis, 2008.
9. Apisakkul, K.T., and Kittichaikarn, C. (2005). Numerical analysis of flow over car spoiler. Paper presented The Ninth Annual National Symposium on Computational Science and Engineering Papers ANSCSE-9, Bangkok, Thailand.
10. Desai M., Channiwala S. A., Nagarsheth, H. J. (2008). Experimental and Computational Aerodynamic Investigations of a Car. *WSEAS Transactions on Fluid Mechanics* Issue 4, Volume 3, 359-366.
11. Hu, Xu-xia., and Wong, E.T.T. (2011). A Numerical Study On Rear-spoiler Of Passenger Vehicle. *World Academy of Science, Engineering and Technology*, 57, 636-641.
12. Lokhande, B., Sovani, S., and Khalighi, B. (2003). Transient simulation of the flow field around a generic pickup truck. SAE Technical Paper Series, 01-1313, 1- 19.
13. Perzon, S., and Davidson, L. (2000). On transient modeling of the flow around vehicles using the Reynolds equation. *International Conference on Applied Computational Fluid Dynamics (ACFD) Beijing China*, 720-727.
14. Vaghela, K. (2013). Optimization of Roof Fairing Angle to Reduce the Aerodynamic Drag of Heavy Duty Truck. *International Journal of Emerging Technologies in Computational and Applied Sciences IJETCAS*, 13-322, 113-117.
15. Solmaz, H., İcingur, Y. (2015). Drag Coefficient Determination Of A Bus Model Using Reynolds Number Independence, *IJAET*, 4 (3) 146-151.
16. Sarı, M,F. (2007). The Aerodynamic Analysis of Air Resistance Affecting the Front Form of Light Commercial vehicles And Its Effect on Fuel Consumption ion. Osmangazi University, Institute of Science and Technology, Master Thesis, Eskişehir, 28-54.
17. Modi, V.J., Hill, S.St. and Yokomimizo, T. (1995). Drag reduction of trucks through boundary-layer control. *Journal of Wind Engineering and Industrial Aerodynamics* 54/55, 583-594.
18. McCallen, R., Flowers, D., Owens T.D., Owens, J., Browand, F., Hammache, M., Leonard, A., Brady, M., Salari, K., Rutledge, W., Ross, J., Storms, B., Heineck, J. T., Driver, D., Bell, J., Walker, S., and Zilliac, G. (2000). Aerodynamic drag of heavy vehicles class 7-8: simulation and benchmarking. SAE Technical Paper Series, 01-2209, 1-19.
19. Ogburn, M.J., and Ramroth L.A. (2007). A truck efficiency and GHD reduction opportunities in the Canadian Truck Fleet (2004-2007). Rocky Mountain Institute Report, Canadian, Canadian, 1-13.
20. Özel, M., Aygün, E., Akansu, Y.E., Bayındırlı, C., Seyhan, M. (2015). The Passive Flow Control around a Truck-Trailer Model.

International Journal of, Automotive Engineering and Technologies, Vol. 4, Issue 4, pp. 185 – 192.  
21. Akansu, Y.E., Bayındırlı, C., Seyhan, M. (2016). The Improvemet Of Drag Force On A Truck Trailer Vehicle By Passive Flow Control Methods, Journal of Thermal Science and Technology, 36, 1, 133-141.